Wave representation of geometrical laser beam trajectories in a hemiconfocal cavity

Y. F. Chen,* C. H. Jiang, Y. P. Lan, and K. F. Huang
Department of Electrophysics, National Chiao Tung University, Hsinchu, Taiwan, Republic of China
(Received 5 December 2003; revised manuscript received 2 February 2004; published 10 May 2004)

We use quantum-mechanics formalism to explore the formation of geometrical laser beam trajectories in a hemiconfocal cavity. Theoretical analysis reveals that laser modes localized on geometrical trajectories are formed by a frequency locking of nondegenerate transverse modes with different longitudinal orders. An experiment is performed to validate the theoretical analysis.

DOI: 10.1103/PhysRevA.69.053807 PACS number(s): 42.60.Jf, 42.60.Da

I. INTRODUCTION

The spatial distribution in a general two-mirror laser resonator is commonly described in term of Hermite-Gaussian (HG) modes of the paraxial wave equation [1]. However, when the optical cavity is hemiconfocal, the dominating mode may be usually not any one of the pure HG mode but can be alternatively viewed as multibounce Gaussian beams traveling in closed off-axis trajectories [2,3]. In other words, the spatial distributions in a hemiconfocal cavity of high Fresnel number are well localized on the geometrical periodic trajectories, as shown in Fig. 1. The periodic trajectories can be characterized by the initial position z_s that is assumed to be on the z axis. The trajectories in Figs. 1(b) and 1(c) are typical periodic orbits, whereas the trajectories in Figs. 1(a) and 1(d) are limiting periodic orbits in the shapes of the letters M and W. Although geometrical optical can be used to find the periodic trajectories in a hemiconfocal acvity, the physical origin of the wave distributions related to geometrical periodic trajectories is unexplored so far. A similar phenomenon in open quantum ballistic cavities is that the striking observation of conductance fluctuations is associated with quantum wave distributions localized on classical periodic orbits [4–6]. In view of that, to establish the relation between the wave distributions and geometrical trajectories it is important not only for understanding laser modes in a degenerate cavity but also for providing analogous insight into the quantum ballistic transport in mesoscopic systems.

In this work, we use quantum-mechanics formalism to analytically construct the wave representation for the geometrical periodic trajectories in a hemiconfocal laser cavity. The formation of geometrical laser beam trajectories is found to arise from a cooperative freuency locking of HG modes with different transverse and longitudinal orders. In the experiment, we demonstrate a diode-end-pumped microchip laser to confirm the theoretical model. Experimental observations show a fairly good agreement with the theoretical predictions.

*Corresponding author. Mailing address: Department of Electrophysics, National Chiao Tung University, 1001 TA Hsueh Road, Hsinchu, 30050, Taiwan. FAX: (886-35) 729134. Email address: yfchen@cc.nctu.edu.tw

II. WAVE REPRESENTATION FOR THE GEOMETRICAL PERIODIC TRAJECTORIES

The interrelation between wave optics and geometric optics is somewhat similar to that between quantum mechanics and classical mechanics [7]. This relation implies that the connection between rays and waves can be explored by use of quantum-mechanics formalism. Recently, the representation of the (2) coherent states have been successfully used to make a connection between the quantum wave functions and the classical trajectories in a two-dimensional harmonic oscillator with commensurate frequencies [8–10]. Here we use the algebra of coherent state to represent the laser modes related to geometric periodic trajectories in a hemiconfocal resonator.

With the paraxial wave equation, the HG $\mathrm{TEM}_{m,n}$ modes can be written as [1]

$$\Phi_{m,n}^{(\mathrm{HG})}(x,y,z) = \frac{1}{\sqrt{2^{m+n-1} m\,!\, n\,!\, \pi}} \frac{1}{w(z)} \times H_m\left(\frac{\sqrt{2}x}{w(z)}\right) H_n\left(\frac{\sqrt{2}y}{w(z)}\right) \exp\left[-\frac{(x^2+y^2)}{w(z)^2}\right] \times \exp\left\{ i\left[\frac{k(x^2+y^2)}{2R(z)} - (m+n+1)\tan^{-1}\left(\frac{z}{z_R}\right)\right]\right\}, \quad (1)$$

where $H_n(\cdot)$ is a Hermite polynomial of order n, the Rayleigh length z_R, the beam radius $w(z)$, and the radius of curvature $R(z)$ are given by

$$z_R = \tfrac{1}{2} k w_o^2, \quad w(z) = w_o \sqrt{1+\left(\frac{z}{z_R}\right)^2}, \quad R(z) = z\left[1+\left(\frac{z_R}{z}\right)^2\right]. \quad (2)$$

Here $k = 2\pi/\lambda$ is the wave number and w_o is the beam radius at the waist. The resonance frequencies of the HG $\mathrm{TEM}_{m,n}$ modes are given by [1]

$$\nu_{\ell,m,n} = \ell(\Delta\nu_L) + (m+n+1)(\Delta\nu_T), \quad (3)$$

where ℓ is the longitudinal-mode index, m and n are the transverse-mode indices, $\Delta\nu_L$ is the longitudinal-mode spacing, and $\Delta\nu_T$ is the transverse-mode spacing. In a planocon-

 ©2004 The American Physical Society

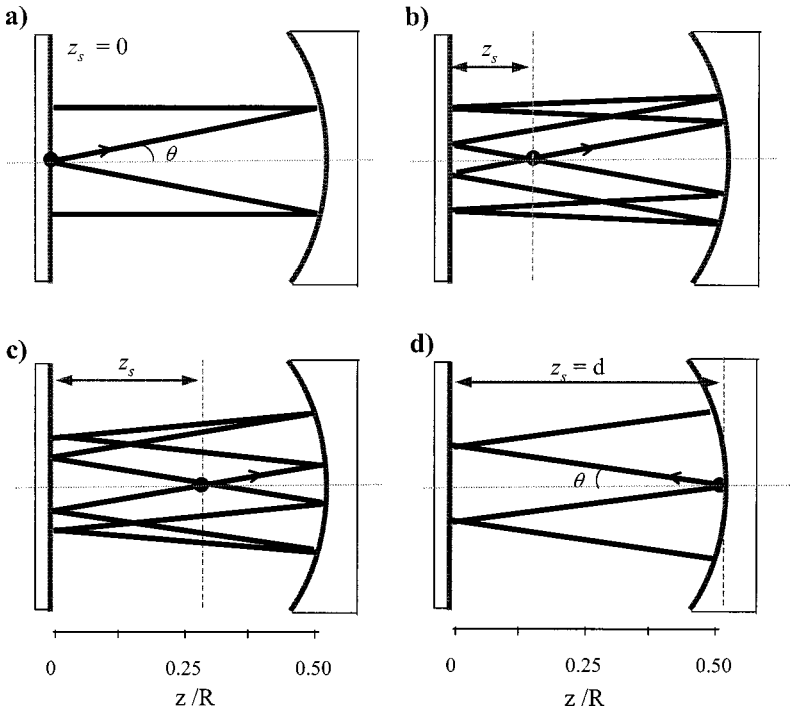

FIG. 1. Geometrical laser beam trajectories in a hemiconfocal cavity; (a) W mode, (b) and (c) typical periodic orbits, (d) M mode.

cave cavity, as shown in Fig. 1, the transverse-mode spacing is given by

$$\Delta\nu_T = \Delta\nu_L\left[\frac{1}{\pi}\cos^{-1}\left(\sqrt{1-\frac{d}{R}}\right)\right], \tag{4}$$

where d is the effective cavity length and R is the radius of curvature of the output coupler. In a hemiconfocal cavity, the cavity length $d=R/2$ deads to the ratio $\Delta\nu_L/\Delta\nu_T=4$. From Eq. (4), it can be seen that lowering (raising) the longitudinal-mode index ℓ by K, while simultaneously raising (lowering) the sum of the transverse-mode indices $m+n$ by $4K$, will leave the frequency unaltered. In other words, a hemiconfocal cavity has a high degree of frequency degeneracy. It has been shown that configurations with a high degree of frequency degeneracy allow closed geometric trajectories [11], as displayed in Fig. 1.

Considering the transverse order in y coordinate to be fundamental mode, a family of the HG modes $\Phi^{(\mathrm{HG})}_{4K,0}(x,y,z)$ in a hemiconfocal cavity can be found to be frequency de-

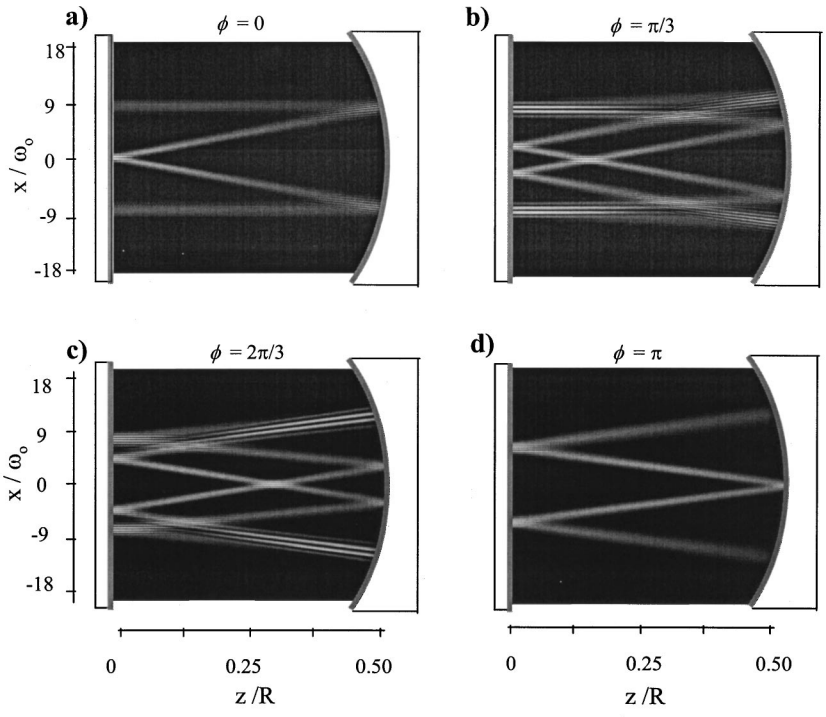

FIG. 2. Dependence of the wave pattern $|\Psi_N(x,0,z;\phi)|^2$ on the parameter ϕ for $N=35$. The wave patterns correspond to the geometrical trajectories shown in Fig. 1.

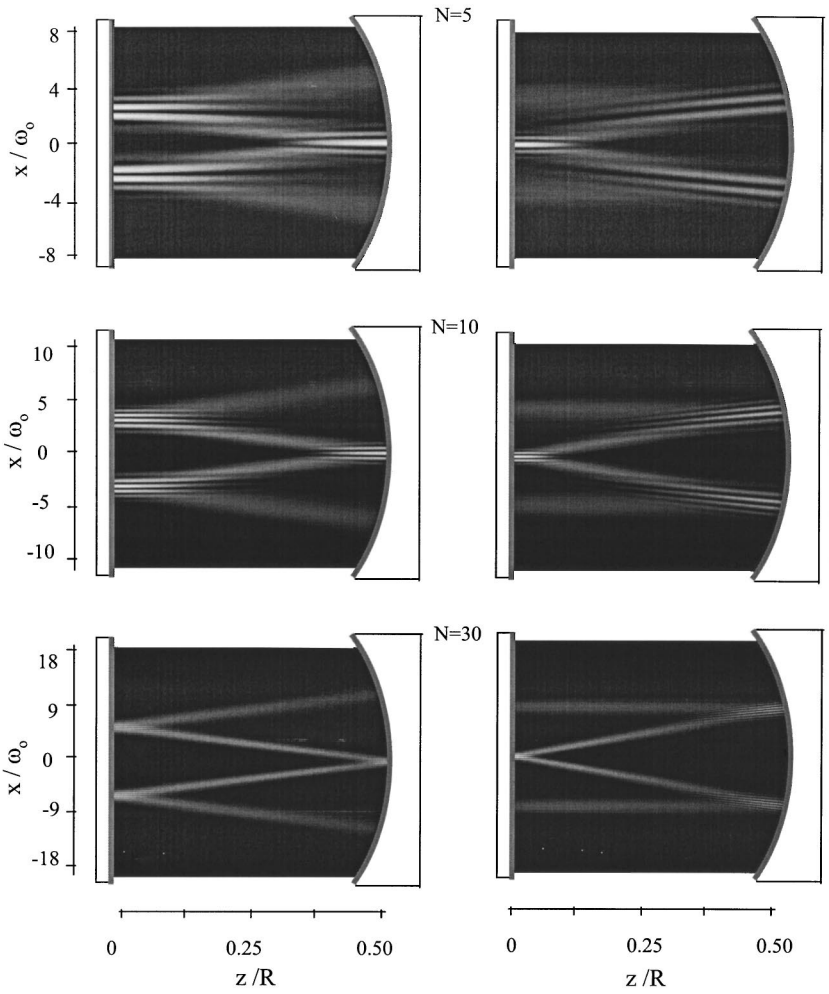

FIG. 3. The N dependence of the wave distributions $|\Psi_N^{(M)} \times(x,0,z)|^2$ and $|\Psi_N^{(W)}(x,0,z)|^2$.

generate by a different longitudinal order $\ell=\ell_o-K$ with a given index ℓ_o. As in the Schwinger representation of the su(2) algebra [8–10,12,13] for a family of the HG modes $\Phi_{4K,0}^{(\mathrm{HG})}(x,y,z)$, where $K=0,1,2,\ldots,N$, the coherent state is given by

$$\Phi_N(x,y,z;\tau)=\frac{1}{(1+|\tau|^2)^{N/2}}\sum_{K=0}^{N}\binom{N}{K}^{1/2}\tau^K\Phi_{4K,0}^{(\mathrm{HG})}(x,y,z), \tag{5}$$

where the parameter τ is, in general, complex and has relation to the geometrical trajectory. For further analysis, the parameter τ is expressed as the polar representation, i.e., $\tau=A\exp(i\phi)$, where the phase factor ϕ is in a range of $[-\pi,\pi]$ and the amplitude factor A is a positive real value. The coherent state is Eq. (2), can be found to have the asymptotic behavior

$$\Phi_N(x,y,z;\tau)\sim\begin{cases}\Phi_{0,0}^{(\mathrm{HG})}(x,y,z) & (A\to 0),\\ \Phi_{4N,0}^{(\mathrm{HG})}(x,y,z) & (A\to\infty).\end{cases} \tag{6}$$

Nevertheless, the structure of wave localization is generally insensitive to the amplitude factor A in the range of 0.5–2. Hereafter the amplitude factor A is set to be unit for the following analysis unless otherwise specified.

As found in different physical systems [14,15], the phase factor ϕ has a causal relationship with the localization on the geometrical trajectories. From numerical analysis, the wave functions related to the geometrical periodic orbits in a hemiconfocal are found to be given by the superposition of two coherent states with the phase factor in opposite sign, i.e., $\Phi_N(x,y,z;e^{i\phi})+\Phi_N(x,y,z;e^{-i\phi})$. As a consequence, the normalized wave function for the geometrical trajectories is given by

$$\Psi_N(x,y,z;\phi)\frac{1}{\left[\sum_{K=0}^{N}\binom{N}{K}\cos^2(K\phi)\right]^{1/2}}\times\sum_{K=0}^{N}\binom{N}{K}^{1/2}\cos(K\phi)\Phi_{4K,0}^{(\mathrm{HG})}(x,y,z), \tag{7}$$

where the range of the parameter ϕ becomes $[0,\pi]$ because $\cos(K\phi)$ in Eq. (7) is an even function of ϕ. Figure 2 depicts the dependence of the wave pattern $|\Psi_N(x,0,z;\phi)|^2$ on the parameter ϕ for $N=35$. It can be seen that the behavior of $|\Psi_N(x,0,z;\phi)|^2$ agrees very well with the geometrical periodic orbit shown in Fig. 1 with the relationship of $z_s=d\tan(\phi/4)$. Note that the relation-

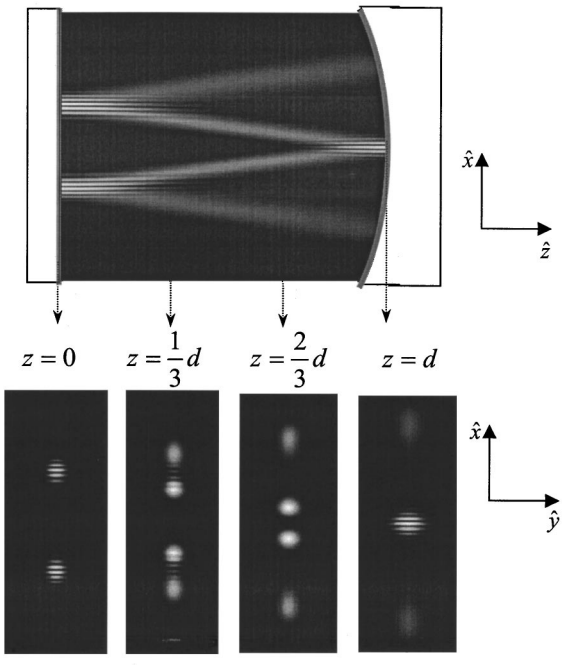

FIG. 4. The transverse intensity profiles at the different longitudinal positions of the cavity for the W mode $|\Psi_N^{(W)}(x,y,z)|^2$ with $N=15$. The corresponding intensity distribution $|\Psi_N^{(W)}(x,0,z)|^2$ is shown in upper for indication.

ship of $z_s=d\tan(\phi/4)$ can be deduced from Eqs. (1), (5), and (7). It is worthwhile to mention that Eq. (7), which gives a connection between the wave functions and geometrical trajectories, is verified from numerical calculations. Even so, the role of the phase factor ϕ can be explored more manifestly from the different physical systems [14,15], namely, quantum billiards in which some of the results are quite similar to the present system.

With Eq. (7), the expressions for the limiting cases of M and W modes can be written as

$$\Psi_N^{(M)}(x,y,z)=\Psi_N(x,y,z;0)=2^{-N/2}\sum_{K=0}^{N}\binom{N}{K}^{1/2}\Phi_{4K,0}^{(\mathrm{HG})}(x,y,z) \tag{8}$$

and

$$\Psi_N^{(W)}(x,y,z)=\Psi(x,y,z;\pi)=2^{-N/2}\sum_{K=0}^{N}\binom{N}{K}^{1/2}(-1)^K\Phi_{4K,0}^{(\mathrm{HG})}\times(x,y,z). \tag{9}$$

The mode index N is related to the divergence angle θ of the mode trajectories as shown in Fig. 1. From wave optics, the divergence angle is given by [16]

$$\langle\theta_x^2\rangle=\frac{\lambda^2}{\pi^2}\int_{-\infty}^{\infty}\int_{-\infty}^{\infty}\left|\frac{\partial\Psi(x,y,0)}{\partial x}\right|^2 dx\,dy, \tag{10}$$

Substituting Eqs. (8) and (9) into Eq. (10), the divergence angle for the Nth order M and W modes is found to be

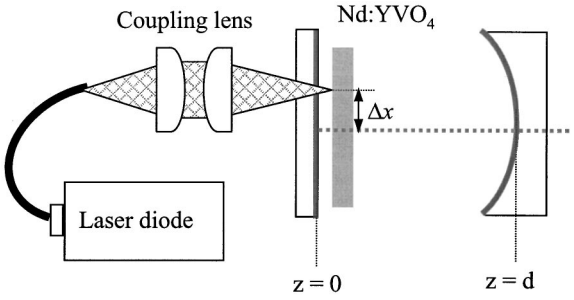

FIG. 5. Experimental setup for the generation of off-axis folded Gaussian beams in a diode-pumped microchip laser with off-axis pumping scheme in a hemiconfocal resonator.

$$\theta_N\equiv\sqrt{\langle\theta_x^2\rangle}=\frac{\sqrt{N+1}}{w_o}\frac{\lambda}{\pi}. \tag{11}$$

Within the paraxial approximation, the divergence angles of higher-order M and W modes, similar to a pure higher-order HG mode, scale with $\sqrt{N}$. More specifically, the result of Eq. (11) comes from the property of the HG modes. Figure 3 shows the N dependence of the wave patterns $|\Psi_N^{(M)}(x,0,z)|^2$ and $|\Psi_N^{(W)}(x,0,z)|^2$. It can be seen that a large order number N is not necessary for the localization of the wave intensities on the geometrical trajectories. Furthermore, the present wave representations manifest that the trajectories between the adjacent order modes are discrete. This result is consistent with the previous observation [3].

It is well known that a pure HG mode is preserved in free-space propagation. However, as shown in Figs. 2 and 3, the laser modes localized on the geometrical rays strongly depend on the longitudinal position. Figure 4 shows the transverse intensity profiles at the different longitudinal positions of the cavity for the W mode $|\Psi_N^{(W)}(z,y,z)|^2$ with $N=15$. The corresponding intensity distribution $|\Psi_N^{(W)}(x,0,z)|^2$ is also shown in Fig. 4 for indication. It can be sent that in the transverse profile on the planar mirror both spots display fringes, whereas in the transverse profile on the spherical mirror only the center peak shows fringes. From the geometrical trajectories, these fringes can be viewed as being the result of interference between two beams overlapping. Therefore, the laser modes localized on the geometrical rays can alternatively be viewed as multibounce Gaussian beams traveling in closed off-axis trajectories.

III. EXPERIMENTAL DEMONSTRATION

In previous works [17,18], off-axis pumping scheme has been successfully used to generate pure high-order HG modes in a general cavity. In the present experiment, we use this off-axis pumping scheme to study the formation of off-axis folded Gaussian beams in a hemiconfocal resonator. As depicted in Fig. 5, the laser cavity consists of one planar Nd:YVO_4 surface, high-reflection coated at 1064 nm and high-transmission coated at 809 nm for the pump light to enter the laser crystal, and a spherical output mirror. The gain medium in the experiment is *a* cut 2.0 at.% Nd:YVO_4 mi-

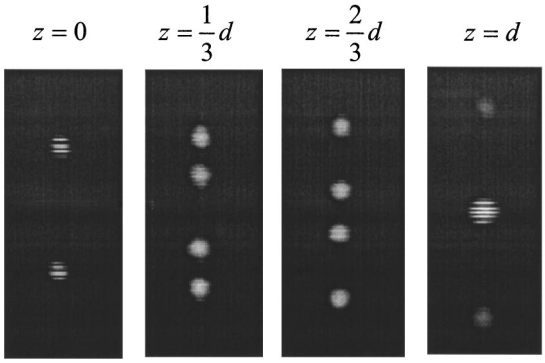

FIG. 6. Experimental results for transverse intensity profiles at the different longitudinal positions of the cavity.

crochip crystal with the length of 1 mm. The absorption coefficient of the $Nd:YVO_4$ crystal is about 40 mm^{-1} at 809 nm. The pump source is a 1-W fiber-coupled laser diode (Coherent, F-81-800C-100) with a 100 μm of core diameter and a numerical aperture of 0.16. Focusing lens with 12.5 -mm focal length and 85% coupling efficiency was used to reimage the pump beam into the laser crystal. The pump radius was estimated to be 25 μm. The radius of curvature of the output mirror is $R=10$ mm and its reflectivity is 98% at 1064 nm.

As expected, pure high-order HG modes were usually observed near threshold in a general cavity length with off-axis pumping. However, the transverse patterns were changed drastically when the resonator length was set to be a hemiconfocal cavity, i.e., $d \approx R/2$. The transverse patterns at the different longitudinal positions of the cavity were measured using a charged-coupled device with a reimage lens. Figure 6 shows the experimental results for transverse intensity profiles at the different longitudinal positions of the cavity. It can be seen that the observed transverse profiles agree very well with the theoretical patterns shown in Fig. 4 for the W mode. The good agreement between the experimental and theoretical patterns confirms that quantum-mechanics formalism can be used to analyze the laser modes localized on geometrical trajectories in a degenerate cavity. Reversely, the optical-mechanical analogy enables one to design the laser resonator for simulating the quantum phenomenon in mesoscopic physics.

We measured the spectral information of experimental W mode by an optical spectrum analyzer (Advantest Q8347). The present spectrum analyzer employs a Michelson interferometer with a Fourier spectrum system to reach the resolution of 0.002 nm. The mode spacing can be found to be 0.028 nm. With the present spectrum analyzer, the mode spectral information can be clearly resolved. The measurement of the optical spectrum reveals the observed W mode to be a single frequency emission. This result evidences that the laser mode localized on geometrical trajectories arises from a spontaneous process of cooperative frequency locking of HG modes with different transverse and longitudinal orders. It is important to distinguish the nondegenerate transverse-mode locking with different longitudinal orders from the degenerate transverse-mode locking in a single longitudinal mode. The degenerate transverse-mode locking leads to the transverse pattern to be preserved in free-space propagation, as a pure HG eigenmode. However, the transverse pattern is significantly different in near-field and far-field regions for a mode formed by the nondegenerate transverse-mode locking. Such a transverse-pattern variation in propagation is caused by the fact that the Gouy phase term $(m+n+1)\tan^{-1}(z/z_R)$ in Eq. (1) is different for the HG modes with different transverse orders. Finally, it is worthwhile to mention that only the W mode can be generated in the present configuration. Applying off-axis pumping scheme to the cavity configuration described in Ref. [3] can generate the M mode in a hemiconfocal cavity.

IV. CONCLUSIONS

In summary, the connection between HG modes and geometric beam trajectories in a hemiconfocal cavity has been analytically constructed by using the su(2) representation of quantum-mechanics formalism. The formation of laser modes localized on geometrical trajectories is found to be a process of nondegenerate transverse-mode locking with different longitudinal orders. The theoretical prediction has been validated with a microchip laser. The good agreement between the experimental and theoretical patterns confirms that optical devices can be used to simulate the quantum phenomenon in mesoscopic physics. For example, electromagnetic wave propagation at microwave or at optical wavelengths has been often considered as a demonstrable model for many quantum-mechanical effects [19–22]. It is believed that the optical-mechanical analogy will continue to be exploited for understanding the physics of mesoscopic systems.

[1] A. E. Siegman, *Lasers* (University Science Books, Mill Valley, CA, 1986).
[2] B. Sterman, A. Gabay, S. Yatsiv, and E. Dagan, Opt. Lett. **14**, 1309 (1989).
[3] D. Dick and F. Hanson, Opt. Lett. **16**, 476 (1991).
[4] R. Akis and D. K. Ferry, Phys. Rev. B **59**, 7529 (1999).
[5] I. V. Zozoulenko and K. F. Berggren, Phys. Rev. B **56**, 6931 (1997).
[6] I. V. Zozoulenko, R. Schuster, K. F. Berggren, and K. Ensslin, Phys. Rev. B **55**, R10 209 (1997).
[7] L. D. Landau and E. M. Lifshitz, *Quantum Mechanics*, 3rd revised ed. (Butterworth Heinemann, London, 2002).
[8] S. De Bièvre, J. Phys. A **25**, 3399 (1992).
[9] J. Pollet, O. Méplan, and C. Gignoux, J. Phys. A **28**, 7282 (1995).
[10] Y. F. Chen and K. F. Huang, J. Phys. A **36**, 7751 (2003).
[11] I. A. Ramsay and J. J. Degnan, Appl. Opt. **9**, 385 (1970).
[12] V. Bužek and T. Quang, J. Opt. Soc. Am. B **6**, 2447 (1989).

[13] J. Banerji and G. S. Agarwal, Opt. Express **5**, 220 (1999).
[14] Y. F. Chen, K. F. Huang, and Y. P. Lan, Phys. Rev. E **66**, 066210 (2002).
[15] Y. F. Chen and K. F. Huang, Phys. Rev. E **68**, 066207 (2003).
[16] N. Hodgson and H. Weber, *Optical Resonators* (Springer-Verlag, Berlin, 1997).
[17] H. Laabs and B. Ozygus, Opt. Laser Technol. **28**, 213 (1996).
[18] Y. F. Chen, T. M. Huang, C. F. Kao, C. L. Wang, and S. C. Wang, IEEE J. Quantum Electron. **33**, 1025 (1997).
[19] S. Longhi, D. Janner, M. Marano, and P. Laporta, Phys. Rev. E **67**, 036601 (2003).
[20] V. Doya, O. Legrand, F. Mortessagne, and C. Miniatura, Phys. Rev. Lett. **88**, 014102 (2002).
[21] L. Sirko, P. M. Koch, and R. Blümel, Phys. Rev. Lett. **78**, 2940 (1997).
[22] R. Morandotti, U. Peschel, J. S. Aitchison, H. S. Eisenberg, and Y. Silberberg, Phys. Rev. Lett. **83**, 4756 (1999).